

Assessment of Next Generation Airframe Noise Prediction Methods with PAA and ASN Flight Test Data

Yueping Guo¹ and Russell H. Thomas¹
NASA Langley Research Center, Hampton, VA 23681, USA

This paper presents an assessment of the airframe noise prediction methods in the research version of the NASA Aircraft Noise Prediction Program (ANOPP) with the objective of validating the accuracy of the current methods, and more importantly, identifying potential improvements to update the methods. The assessment compares predictions of the individual noise components currently implemented in ANOPP, including the landing gear, the slat, the flap, and the trailing edge noise, with the data from the Propulsion Airframe Aeroacoustics and Aircraft System Noise flight test conducted as part of the Boeing 2020 ecoDemonstrator program on a Boeing 787-10 Etihad Airways aircraft. For each component, prediction errors and discussions are presented for the noise characteristics, covering not only the source features but also the installation effects. It is shown that the predictions capture the major noise features, but improvement potential is identified in two main categories. The first includes minor features that have not been sufficiently modeled in the current methods, the noise due to interactions of the landing gear wake with the flaps and the slat bracket noise, for example. The second is related to changes in modern aircraft designs, which may alter the noise source mechanisms, and thus, calls for major improvements and updates on the current prediction models, examples including the flap side edge noise for modern flap systems and the trailing edge noise for realistic wings with taper and sweep. To illustrate the progress of the method development, previous generations of airframe noise models in ANOPP are also compared with the flight test data.

I. Introduction

The capabilities and methodologies of airframe noise prediction have been continuously evolving, not only because of the improvements in understanding the noise source mechanisms, but also due to the need to account for the continuously changing aircraft design features that may alter the source characteristics and/or introduce new sources. A well-known example of the former is the slat and the flap noise models changing from early methods based on the trailing edge noise theory [1], [2] to more physics-based methods [3]-[5] that capture the characteristics of flow noise related to the slats and the flap side edges, respectively. An example of the latter is the continuous progress in aircraft high-lift system design, which has seen complex multielement flaps in old aircraft replaced by simple, smooth single-element flaps in recent generations of aircraft. The flap noise prediction models, of course, need to be in step with this progress because of the changes in noise sources associated with the design changes. The changes in flap configuration can also affect other noise components, because of the installation effects that couple all airframe noise components to the high-lift system, aerodynamically and/or acoustically. Even the landing gear noise component, which is itself not a high-lift element, is strongly affected by the changes in flap design; its source strength is correlated to the local flow velocity below the high-lift system, and its propagation to the far field is modified by the reflection from the high-lift element surfaces and by the refraction of the local nonuniform mean flow [6].

The needs for improvements and updates in the prediction methods, of course, start with thorough reviews and assessments of the methods currently in use [7]-[11]. This is the objective of the research in this paper. A critical assessment and analysis will be presented for the next generation airframe noise prediction methods currently implemented in the research version of the NASA Aircraft Noise Prediction Program (ANOPP-Research), which will be facilitated by comparing the predictions with data from the Propulsion Airframe Aeroacoustics (PAA) and Aircraft System Noise (ASN) flight test, using the Etihad Airways Boeing 787 ecoDemonstrator aircraft [12], [13], for all the airframe noise components, including the landing gear, the slat, the flap, and the trailing edge noise. The methods in ANOPP-Research have been validated before, mostly on a component basis as each individual component model is

¹ Senior Research Engineer, Aeroacoustics Branch, AIAA Associate Fellow.

developed. The assessment with the Boeing 787-10 aircraft data in this paper will provide a systematic validation by data from a full configuration aircraft in flight. Validation of component noise prediction by flight test data is by no means an easy task because the aircraft cannot fly with only one airframe component deployed, at least not at realistic flight conditions such as altitude, engine power and flight speed. This is made feasible here because a subset of the flights is dedicated to airframe noise prediction validation with a carefully planned test matrix that allows the component noise to be extracted by combining data sets from various flights. The comparisons between data and predictions will demonstrate the accuracy of the methods, and, more importantly, will identify potential improvements by analyzing features for which the comparisons between data and predictions reveal noticeable errors.

The prediction methods in the ANOPP framework for the major airframe contributors, namely, the landing gear, the slat, and the flap noise component, have been through three generations. The first is the Fink method, developed for all the airframe noise components and implemented in the 1970s [1]-[2], referred to as ANOPP-Fink. This is mostly an empirical method heavily relying on calibrations for the noise amplitudes by wind tunnel and flight test data available at that time. For parametric trends, the method uses models of simple and idealized configurations. Insufficient understanding of the source mechanisms and incorrect models in various parametric trends started to be recognized in the early 2000s, which, together with the availability of more test data for both component and total airframe noise, has led to a generation of prediction methods based on more physics of the sources for the airframe components [3]-[6], [15]. These are implemented in ANOPP as the Boeing airframe noise method, referred to as ANOPP-BAF, and can be considered as the second generation of airframe noise prediction methods in ANOPP. Starting from 2015, a series of updates has been developed, both to improve the accuracy of ANOPP-BAF and to extend its functionalities to account for features and/or components that were not captured in the original methods of ANOPP-BAF [16], [17]. Interactions between components, reflection from the airframe, for example, have also been significantly improved. These improved and extended methods are implemented as ANOPP-Research and can be considered as the third generation of airframe noise methods. They follow the same methodology as in BAF, namely, the physics-based modeling, with significant improvements in accuracy, functionality, and applicability. For example, while ANOPP-BAF is mostly suitable for conventional aircraft configurations of tube and wing design, the new set of methods in ANOPP-Research can be used for unconventional aircraft configurations, such as the hybrid wing body (HWB) aircraft [19] and the truss braced wing aircraft [20] that have very different airframe configurations from the conventional design.

Because the airframe noise models in ANOPP-Research are developed based on flow physics and source mechanisms, it can be expected, and will be shown, that the major features in the component noise, such as the noise spectral shape, the source polar directivity, the dependencies on the flow Mach number, and the correlations of the component noise with the component geometry, are sufficiently captured by the prediction models. The validation will show that the component models for the landing gear noise and the slat noise have sufficient overall accuracy with only small discrepancies between data and predictions. The errors will be discussed and attributed to minor features that are not included in the current prediction models. For flap noise, it will be shown that the parametric trends are sufficiently captured, but the noise amplitude is overpredicted. The overpredictions are attributed to the insufficient modeling of the current flap noise amplitude model in ANOPP-Research to account for the smooth geometric variations of the flap systems for the Boeing 787 aircraft, which are very different from the multielement flap systems in prior aircraft types for which the flap noise model was originally developed [3]. This is identified as a potential major improvement.

Another potential major improvement identified by the assessment is the trailing edge noise component, for which the prediction method has not been updated since its original development [1], [2]. The lack of updates in the prediction method has been justified and attributed to the minor contributions of this component to the total airframe noise for conventional aircraft. This is still true. The renewed interests in this component in recent years [21] result from its potential applications in unconventional aircraft [19], [20]. The assessment for this component is feasible because the flight tests include clean wing configurations for which the trailing edge noise is the main component. Large errors will be shown by comparisons with data, because of the prediction methodology not being in step with the aircraft design.

To illustrate the progress of the method development in the ANOPP framework, comparisons and discussions will also be presented for previous generations of airframe noise prediction methods in ANOPP, for the landing gear, the slat, and the flap noise component, which have been through various updates and improvements over the past few decades. It will be shown that the most significant improvements have resulted from the changes in prediction methodology from heavily empirical methods to more physics-based methods, leading to not only more accurate predictions at typical landing configurations for conventional aircraft, but also extended prediction functionalities that are required for variations in aircraft and/or high-lift system design.

II. Test Setup and Data Processing

The database used in the analysis in this paper is from a subset of the flights overviewed in [12] and [13] so that only the details relevant to airframe noise analysis are described here to facilitate the discussions. The test was carried out at the Boeing flight test site in Glasgow, Montana, which is known for its favorable environment for acoustic testing, using a Boeing 787-10 Etihad Airways aircraft. The aircraft at its landing configuration is shown in Fig. 1. The subset of the test matrix for airframe noise is designed to have minimal engine noise by operating the engines at idle power settings. The test conditions are chosen to ensure good signal to noise ratio and to allow for the extraction of component noise. There are extensive acoustic measurements in the flight tests, including on-board near field measurements and far field measurements on the ground. The latter is the most relevant to airframe noise and includes a phased microphone array and a series of individual microphones. The focus of this paper is the individual microphone data, while the analysis of the phased array data will be left to a future study.



Fig. 1 Boeing 787-10 aircraft used in the NASA/Boeing flight test. Photo Credit: The Boeing Company.

The layout of the individual ground microphones is illustrated in Fig. 2. The measurement locations cover eight positions in the lateral direction, including the flyover plane and covering the lateral position for noise certification. At each lateral position, a few microphones are placed in the flight direction to facilitate ensemble averaging. The directivity pattern in polar angle is achieved using the measurements along the flight path, while the directivity in the lateral direction is provided by the measurements at the eight lateral stations, of which the measurements in the flyover plane are used for the analysis in this paper. The separation of the microphones in the flight direction is designed to have statistically independent measurements, while maintaining minimal changes in source features. The microphones are installed on base plates that are designed by Boeing to mimic rigid surface reflection and minimize edge interference. Thus, the ground reflection correction is simple, and the free field noise can be easily derived by subtracting 6 dB from the measured data.

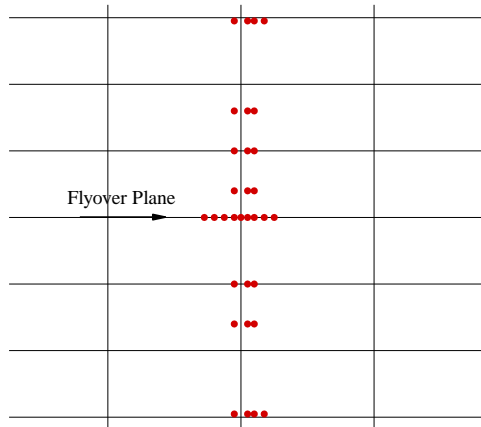


Fig. 2 Individual microphone layout.

The test conditions for the airframe noise flights are defined according to the high-lift system settings of the Boeing 787-10 aircraft, which contain variations in the flaps and the slats. These variations are combined with the landing gear positions. The conditions are summarized in Table 1, where the first column is the detent of the high-lift system, with the second and the third columns listing the corresponding positions of the flaps and the slats, respectively, and the last column shows the landing gear position. The numbers in the figure are identifications of the positions, not the

actual deployment angles. For each detent setting, the flaps and the slats have their individual positions, and the landing gears can be deployed or retracted. This gives a total of ten configurations, each of which has at least two flights.

Table 1 High-lift system and landing gear positions for airframe noise flights.

Detent	Flap Position	Slat Position	Landing Gear Position
0	1	0	Up and Down
1	1	1	Up
5	2	1	Up
20	4	1	Up and Down
25	4	2	Up and Down
30	5	2	Up and Down

The data processing consists of two phases. The first phase is the correction and normalization of the data to a common flight path and acoustic standard day. The data analysis and component extraction involve pairs and/or groups of flights that are designed to have the same target flight conditions, their flight paths and flight speeds, for example. Small deviations from the targets are, however, inevitable, so that the data sets need to be corrected for the flight condition deviations. The correction for the sound propagation distance, varying with the flight paths, is done by normalizing the flight paths to a standard path with the inverse square law for the propagation distance, while keeping the emission angle the same. This provides a uniform normalization for all the individual datasets. This phase of the data processing is integrated into the data acquisition and reduction performed by Boeing using its in-house standard procedures, including the conversion of the time domain measurements to spectra. The data are corrected for the ground reflection so that the results are all free field noise. All airframe noise datasets are normalized to a common flight path with a 3-degree downward slope, an overhead altitude of 600 feet, and a nominal flight speed of 155 knots. The nominal flight speed is used to determine the source positions on the common flight path with the same set of emission angles as those on the as-flown path. At the new source positions on the common path, the effect of propagation distance is corrected by the inverse square law for the spectra and the atmospheric absorption is corrected to the standard acoustic day conditions of 70% relative humidity and 77 degrees Fahrenheit temperature. These are all propagation effects, easily corrected for all datasets.

The second phase of the data processing involves corrections and normalizations that depend on individual components and on the purpose of the data analysis. These are involved in the component extraction and may include the source strength changes with the flight speed and the Doppler effects of amplitude amplification and frequency shift. An example of the component-dependent correction is the source strength variations with the flight speed, which may differ between various noise components. For the extraction of a specific noise component, all flight datasets used in the extraction process are corrected to the same conditions. The extraction may involve two or more flights and is done on the acoustic energy basis, assuming all the noise sources are incoherent. The extracted component noise datasets are listed in Table 2, together with the corresponding settings of the aircraft configurations.

Table 2 Noise components extracted from flight test data.

Noise Component	Gear Setting	Slat Setting	Flap Setting
	Down	Cruise	Cruise
Landing Gear	Down	Takeoff	Takeoff
	Down	Landing	Landing
Slat	Up	Takeoff	Cruise
	Up	Landing	Cruise
Flap	Up	Cruise	Takeoff
	Up	Cruise	Landing
Trailing Edge	Up	Cruise	Cruise

The deployment and the retraction of the landing gears are denoted respectively by the “down” and the “up” setting in the table. The high-lift elements, namely, the slats and the flaps, have their respective takeoff and landing setting. In addition, they are denoted by the cruise setting if not deployed. There are altogether eight unique configurations for the four noise components. The datasets are 1/3 octave band spectra for emission angles from 15 to 165 degrees at a 5-degree increment and are for the eight measurement locations in the lateral direction, shown in Fig. 2. The data are the ensemble-averaged results for each of the microphone groups shown in the figure.

III. Landing Gear Noise

Over the past few decades, prediction methods for aircraft landing gear noise have been updated multiple times. The original method used in ANOPP is an empirical model entirely based on small-scale simple model test data [1], [2] and was shown later to greatly underpredict the noise levels of real landing gears [15]. Because of this, the method was replaced by another empirical model based on wind tunnel test data of the Boeing 737 landing gear [23], necessarily an isolated gear without the installation effects of the high-lift system, but a full-scale and full-configuration gear with all realistic details. The empirical model was later replaced again by a more general method based on component modeling of the source mechanisms [15], which decomposes the landing gear noise into the low-, the mid- and the high-frequency components, corresponding to the noise sources respectively associated with the wheels, the struts, and the small parts in the gear assembly. In the development process, it was recognized that the local flow around the gears can significantly affect the noise levels [6], [22], because the noise levels are scaled on the sixth power of the local flow velocity, which is influenced by the high-lift system. The local flow velocity is known to be smaller than the free stream velocity and is quantified for noise prediction in a parametric study. In recent years, the reflection of landing gear noise by the wing and the high-lift system was also recognized to be important to the levels and the directivities of the total landing gear noise.

Thus, the current landing gear noise prediction contains models (ANOPP-Research) for both the source characteristics and the installation effects. The former includes spectral features, far field directivity patterns, dependence on flow velocity, and correlations with the geometry of the gear parts, and the latter includes the local flow effects and airframe reflection. In addition, propagation effects, such as the Doppler effects, the propagation distance effects, and the atmospheric absorption, are also accounted for in the prediction method. An illustration of the landing gear noise prediction is given in Fig. 3, which plots the 1/3 octave band sound pressure level (SPL) as a function of frequency for the total gear noise, as well as its three components, respectively from the wheels, the struts, and the small parts.

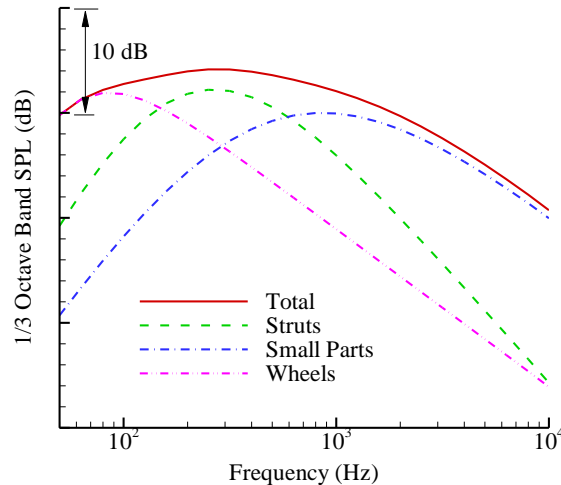


Fig. 3 Typical landing gear noise spectrum and its composition.

For the Boeing 787 aircraft, the accuracy of the spectral predictions by ANOPP-Research is shown in Fig. 4, for the cruise wing and the landing high-lift setting, respectively, by the left and the right plot in the figure. The accuracy is represented as the differences between predictions and data in the 1/3 octave band Sound Pressure Level (Δ SPL) as a function of frequency and emission angle in the flyover plane. The differences between predictions and data are also referred to as errors in this paper for the convenience of discussions, even though the data may also include measurement uncertainties so that the differences are not exactly errors. The errors are defined to be overprediction for positive Δ SPL and underprediction for negative Δ SPL. The case of cruise wing is where neither the slats nor the

flaps are deployed so that the noise reflection is only from the wings and the local flow effects are small. In comparison, the case of landing high-lift setting is the configuration for noise certification at approach conditions with both slats and flaps deployed at approach settings. The results show errors less than about 2 dB in noise amplitude for most of the important frequencies and emission angles, indicated by the green color.

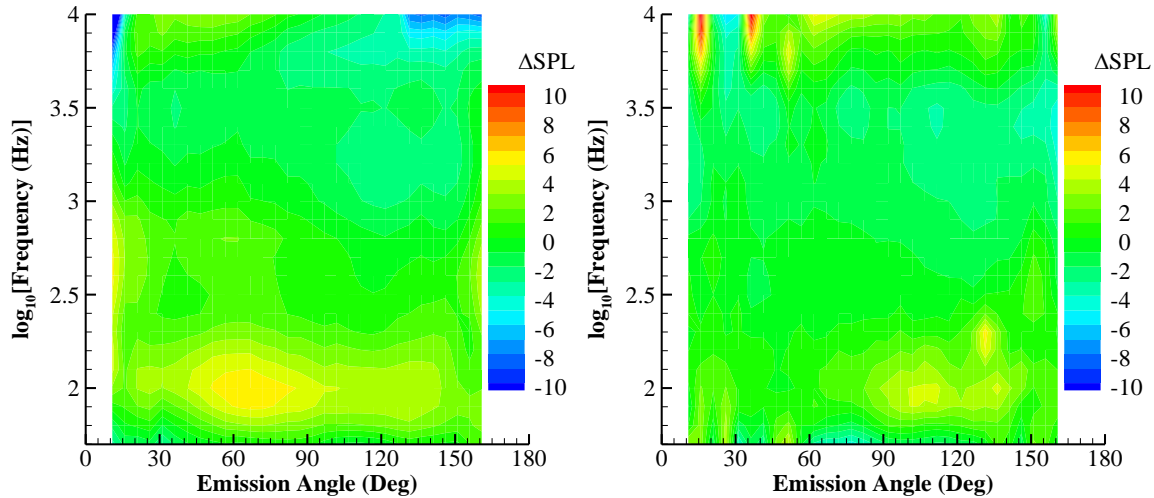


Fig. 4 Prediction accuracy of gear noise spectra for cruise (left) and landing (right) settings in flyover plane.

There are three areas in the contour plots where the errors are larger than 3 dB, either underprediction or overprediction. The first is the high frequency domain above about 6000 Hz where the errors can be large and irregular. These are likely due to the processing of the test data, which usually have much lower levels than the spectral peaks and may introduce large errors in the process of extracting the landing gear noise by incoherent energy subtraction. The large errors, however, have no practical importance because the low levels at the high frequencies make their contributions to the total noise metrics negligible.

The second area of large errors is the low frequency domain around 100 Hz where the overprediction can be up to 6 dB, shown by the yellow patches in the contour maps for many emission angles. These errors are likely due to the use of Strouhal number scaling in the prediction method that determines the peak frequency of the low frequency component by the wheel diameter, assuming that this geometric dimension is proportional to the characteristic length scale of the noise sources. While this assumption, and hence the Strouhal number scaling, can be expected to be applicable for small and intermediate geometric dimensions, the proportionality between the geometric dimension and the source characteristic scale may not be valid at large dimensions, such as the wheel diameter. In this case, the complex structure of the gear assembly and the complex flows around it can prevent the formation of flow features of such a large size. Thus, the low frequency noise due to the wheels needs to be scaled on length scales that are probably smaller than the wheel diameter. This can be a potential improvement of the current method. However, it may only be a minor improvement because the low frequency noise is heavily suppressed in the computation of the certification noise metrics.

Another region of noticeable errors shown in Fig. 4 is the mid-frequency domain around 2000 Hz, for aft emission angles at cruise wing settings and for more angles for landing settings, where underpredictions of up to 4 dB can be seen. It is difficult to pinpoint the causes of these errors by the comparisons alone, but a few likely candidates can be pointed out. One possible cause is the interactions of the turbulent wake flows of the gear assembly with the trailing edges of the wings and/or flaps. This is a feature recently studied [24], [25] and has not been adequately modeled in the prediction method in ANOPP-Research. It is worth noting that this effect is reported to be most pronounced in the mid- and high-frequency domain and in the angles away from the overhead position. This seems to be the case for the results shown in Fig. 4 for the frequencies of the underprediction. Thus, the wake interaction noise may not be completely responsible for the errors in the figures. Another possibility is the locations of the high-frequency sources consisting of small structural elements in the gear assembly, which are the main noise sources in the kilohertz range, as shown in Fig. 3 and are most sensitive to the local flow so that errors in their distribution may cause noticeable errors in the predicted noise levels. This noise component is the most difficult one of the three gear noise components to predict because of the uncertainties in the distribution and dimensions of the structural details. These will be further investigated as part of the efforts to improve the prediction capability.

To demonstrate the accuracy of the gear noise component predictions in the noise certification metrics, the difference between the ANOPP-Research predictions and the flight test data in the tone corrected perceived noise level (PNLT) is plotted in Fig. 5 as a function of emission angle, for both cases of cruise wings and landing settings. This noise metric is calculated on the normalized flight path with overhead altitude of 600 feet and flight speed of 155 knots. The errors in the noise metric of PNLT, plotted in the figure by the symbols, are within about 2 dB for most of the important emission angles. The first emission angle of 15 degrees and the last one of 165 degrees have relatively large errors. These angles, however, have levels below the 10 dB cutoff so that they do not affect the total noise in certification. The errors shown in the figure also demonstrate the accuracy of the directivity modeling. The quantity is not the usual overall sound pressure level (OASPL), but the PNLT, which is more relevant to noise certification with frequency weighting. From the component PNLT, the noise metric of the effective perceived noise level (EPNL) can be calculated for both the predictions and the data. The differences between the two are -0.5 and -1.0 dB, respectively, for the cruise wing and the landing settings. Both are underpredictions and likely due to the underpredictions of the spectra in the mid-frequency domain discussed in relation to Fig. 4.

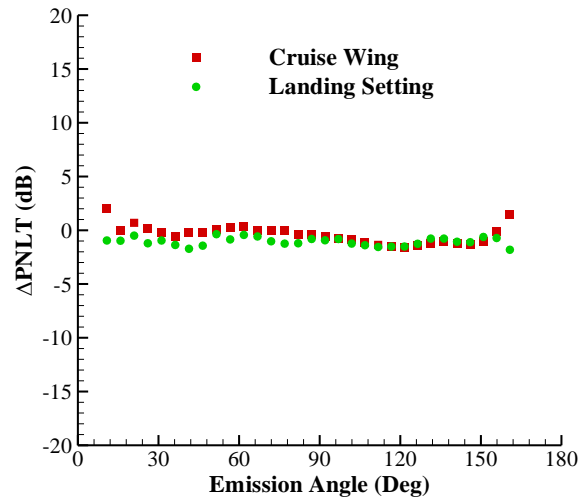


Fig. 5 Prediction errors of gear noise PNLT in flyover plane.

The case of landing gear noise for cruise wing settings is included in the error analysis in this section, obviously not because of its relevance to aircraft noise certification. Instead, it shows the accuracy and versatility of the prediction method at different installation configurations. This is important because the installation effects of noise reflection and source correlation with local flows for landing gear noise are both modeled in the method for applications where the aircraft configuration differs from the conventional designs, such as the trust-braced-wing aircraft [20] and the hybrid-wing-body aircraft [17] that have very different airframe configurations. In these cases, both the noise reflections and the local flow effects are different, requiring the prediction capability to account for the configuration changes.

The prediction errors for the landing gear noise component discussed in the previous paragraphs are summarized in Table 3, where the four columns are respectively for the domains of the errors in terms of frequency and emission angle, the possible causes of the errors, the potential improvements to correct these errors, and the impact of the potential improvements to the total gear noise prediction.

Table 3 Landing gear noise prediction error and potential improvement.

Domain	Possible Cause	Potential Improvement	Impact on Component EPNL
High Frequency (above 6000 Hz)	Measurement Uncertainty	No	None
Low Frequency (below 100 Hz)	Wheel Diameter Scaling	Yes	Minor
Kilohertz Range at Aft Angles	Wake/Edge Interaction, Small Gear Parts	Yes	Minor

IV. Slat Noise

The first method implemented in ANOPP for slat noise prediction is the Fink method [1], [2], based on the trailing edge noise theory with calibrations by data from aircraft noise tests. The method was later commonly recognized as insufficient in accuracy and applicability, mainly because the trailing edge noise theory does not capture the physics of the slat noise sources. It is now commonly known that trailing edges are not significant contributors to slat noise. Instead, the main source mechanisms of slat noise are the cove flow, the gap flow, and the brackets. Based on this improvement of the understanding of source mechanisms, a more physics-based method was developed and implemented in ANOPP [5]. This method was later further extended to Krueger device noise prediction [17], as well as other improvements, leading to the version in ANOPP-Research. An illustration of the spectral prediction by this method is given in Fig. 6, showing the total slat noise SPL, as well as its components. The spectral peak is in the hundred hertz range, correlated to the slat chord length and dominated by the noise generated by the cove flow. The gap flow and the slat brackets generate noise in the mid and high frequency domain, with amplitudes correlated to the respective geometric parameters of the two components, which determine the falloff rate of the total noise spectrum.

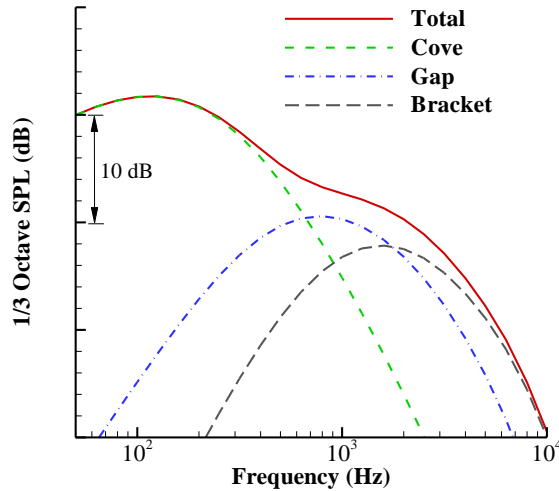


Fig. 6 Typical slat noise spectrum and its composition.

The accuracy of the spectral predictions by ANOPP-Research for the Boeing 787-10 aircraft is illustrated in Fig. 7 with the errors Δ SPL plotted as a function of both frequency and emission angle for the takeoff and the landing slat settings, respectively by the left and the right plot. The large areas of green color in the figures indicate the accuracy of the predictions is within about 2 dB for most of the frequencies, from about 100 Hz to 6000 Hz, and for most of the emission angles, from about 20 to 160 degrees.

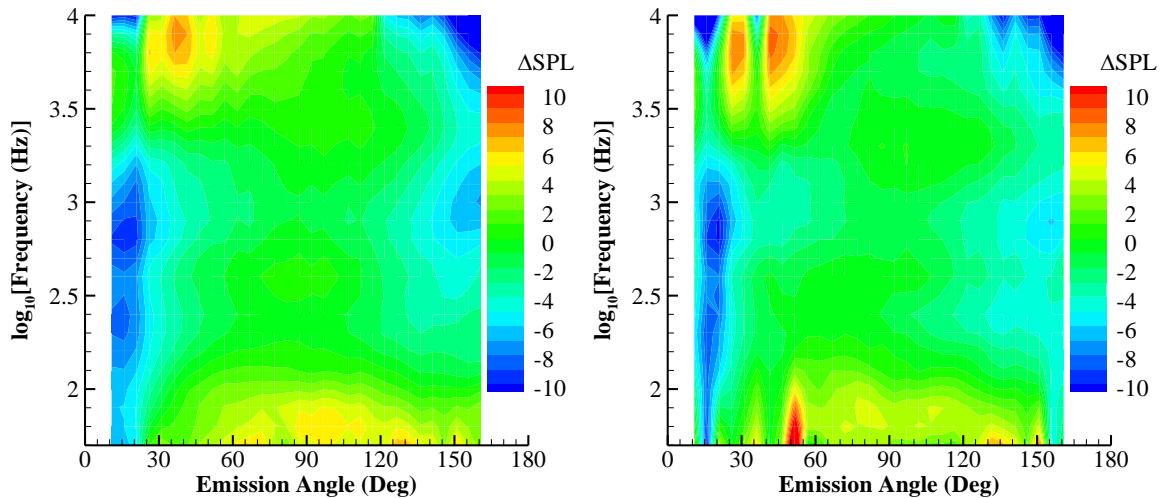


Fig. 7 Prediction accuracy of slat noise spectra at takeoff (left) and landing (right) settings in flyover plane.

There are four identifiable exceptions to the high accuracy of the slat noise prediction. The first is at high frequencies above about 6000 Hz, where, similarly to the case of landing gear noise prediction discussed in the previous section, the errors are large and irregular, underprediction of up to 10 dB at one emission angle and overprediction of up to 10 dB at the next emission angle. These are most likely due to errors in the processing of the flight test data in the extraction of the slat noise component by combining datasets at different conditions and do not have noticeable impact on the total noise metrics because of the low levels of the spectra at these frequencies, as shown in Fig. 6.

The second noticeable large errors are at very small emission angles, below about 20 degrees, where the underpredictions can be up to 10 dB, indicated by the patches of blue color. These are also most likely due to the errors in the data processing because the large propagation distances and the heavy atmospheric absorption at these angles introduce uncertainties in the data. The impact of these large errors is very small, because the noise levels at these angles are very low, compared to the levels at the peak radiation angle. The levels at very small emission angles are likely below the 10 dB cutoff in the calculation of the noise certification metrics. In this case, the errors have no impact at all.

Relatively large errors are also seen in Fig. 7 at low frequencies, below about 100 Hz, in the form of overpredictions of up to 5 dB, represented by the patches of yellow color in the figures, except for the red spike at about 50 degrees, which is again due to measurement uncertainty. As illustrated in Fig. 6, the low frequency slat noise is associated with the cove flow with the spectral peak scaled on the chord length of the slat in the prediction method. For full scale aircraft such as the Boeing 787, the slat chord lengths are large, between 1 to 3 feet, for example. The Strouhal number scaling in the prediction method assumes that the flow features in the cove flow also have the same large characteristic lengths. This may not be an accurate modeling of the cove flow features, which may have length scales smaller than the slat chord, either because the complex geometry and/or the complex cove flow tend to break up the large-scale features, or because the length of the relevant geometric segment that produces the cove flow is not the entire chord. In either case, an improved modeling of the length scale will shift the spectral peak of the low-frequency slat noise to a slightly higher frequency, effectively reducing the noise levels at frequencies on the lower side of the spectral peak. This improvement, however, can be expected to have only a minor impact to the overall slat noise because the low frequency noise is heavily suppressed in the certification metrics.

The results in Fig. 7 also reveal a general trend of underprediction, up to about 4 dB in the kilohertz frequency range, at emission angles far away from the overhead position, especially in the aft quadrant. These differences are likely due to inadequate modeling of the noise directivities for the gap noise and the bracket noise, both being important in the kilohertz range. The modeling of the directivities captures the peak radiation angles very well. The directivity patterns for the components in the slat noise, however, have not been validated and calibrated as well, mostly due to the lack of quality test data. A more gradual falloff of the directivity patterns in the prediction method can help improve the accuracy at large emission angles.

To summarize the noticeable prediction errors for the slat noise component discussed in the previous paragraphs, Table 4 shows the domains of the errors in terms of frequency and emission angle, the possible causes of the errors, the potential improvements to correct these errors, and the impact of the potential improvements to the total slat noise prediction.

Table 4 Slat noise prediction error and potential improvement.

Domain	Possible Cause	Potential Improvement	Impact on Component EPNL
High Frequency (above 6000 Hz)	Measurement Uncertainty	No	None
Very Small Angle (below 20 degrees)	Measurement Uncertainty	No	None
Low Frequency (below 100 Hz)	Cove Chord Length Scaling	Yes	Minor
Kilohertz Range at Aft Angles	Component Directivity	Yes	Minor

The impact of the errors in the spectral predictions to the slat noise component in certification metrics is illustrated in Fig. 8 with Δ PNLT plotted as a function of emission angle for both the takeoff and the landing settings. The errors in EPNL for the two cases are respectively -0.3 and -0.8 dB, both slightly underpredicting and probably within the

variations of data repeatability. This high accuracy is of course not uniformly true for more detailed noise metrics, such as the errors in PNLT plotted in this figure and the spectral prediction errors shown in Fig. 7. By excluding the very small and very large angles where the noise levels are below or close to the 10 dB cutoff for the calculation of EPNL, the errors in PNLT are within 1 dB of the data for forward angles and are up to 3 dB in aft angles.

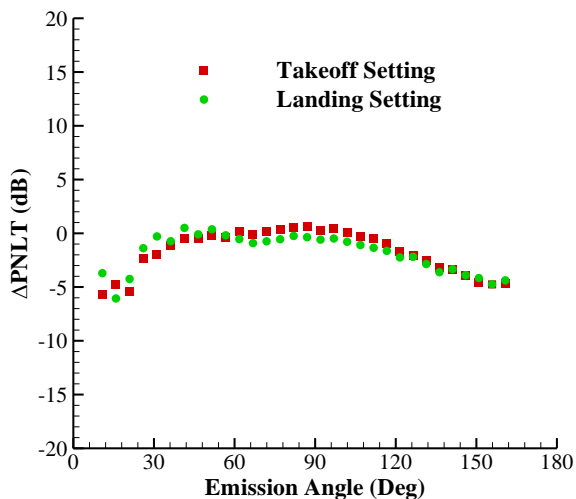


Fig. 8 Prediction errors of slat noise PNLT in flyover plane.

V. Flap Noise

The development of flap noise prediction methods in the ANOPP framework has a similar progress to the slat noise component discussed in the previous section. The progress started with the Fink method [1], [2], based on the trailing edge noise theory with calibrations by available aircraft noise test data. The method was later recognized as insufficient in accuracy and applicability, mainly because the trailing edge noise theory does not capture the physics of the flap noise sources. It is now commonly known that trailing edges are not significant contributors to flap noise, compared with the noise generated at the side edges of the flaps. At the side edges, the rollup vortex interacting with the sharp corners that have radii of curvature much smaller than a typical acoustic wavelength and the fluctuations of the shear layers emanating from the corners have been identified as the main source mechanisms. Based on this improvement of understanding, a more physics-based method was developed and implemented in ANOPP [3], which correlates the far field noise to geometric and operational parameters of the flaps, especially the side edge geometry. This method was later further extended in applicability and improved in accuracy, leading to the version in ANOPP-Research. An illustration of the spectral prediction by this method is given in Fig. 9, showing the total flap noise, as well as its components.

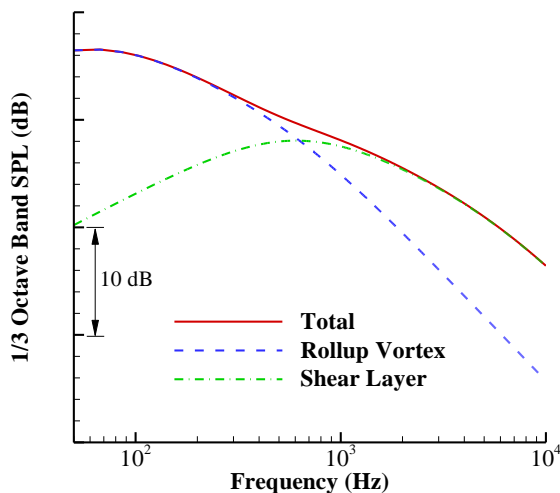


Fig. 9 Typical flap noise spectrum and its composition.

The method in [3] and its subsequent updates have been validated and calibrated by both component model test data and aircraft test data. The latter includes aircraft such as the DC-10, the Boeing 777, and the Boeing 747, all of which have flap systems characterized by multielement configurations with abrupt geometry changes at the side edge locations along the aircraft wingspan. This leads to jumps in spanwise aerodynamic loading at the side edges, which in turn leads to strong rollup vortices and strong shear layers at the side edges, generating significant amounts of side edge noise. For the Boeing 787-10 aircraft, however, the flap systems are noticeably different, with single elements for both the inboard and the outboard flap and with a smooth transition between the two. Intuitively, this should be beneficial to noise. Because of this noise benefit, it can also be expected that prediction methods calibrated to previous designs are likely to overpredict the flap side edge noise. In recognizing this, a temporary correction was implemented in the ANOPP-Research version of the flap noise method, treating the potential noise changes due to advanced flap systems as a uniform noise reduction independent of any parameters. Due to the lack of test data, the amount of the noise reduction has not been validated. Furthermore, the uniform noise reduction in all parameters is not likely to be the case. Thus, the assessment of the prediction accuracy in this section will not use this temporary correction. Instead, the errors revealed by the assessment on the version without the correction will be used to identify the impact of the modern advanced flap systems and to help develop/improve the flap noise models to account for the design changes.

The prediction accuracy of flap noise spectra is shown in Fig. 10, where the errors are plotted as a function of both the emission angle and the frequency, again, for both the takeoff and the landing settings. As discussed in previous sections for the landing gear and the slat noise component, the large and irregular errors at very high frequencies are due to the artifacts in the data processing in the component extraction and do not have any practical impact on the total noise. Also, the large overpredictions at low frequencies below about 100 Hz are likely due to the Strouhal number scaling of the low frequency flap noise based on the flap chord length, which only has a minor impact on the total flap noise.

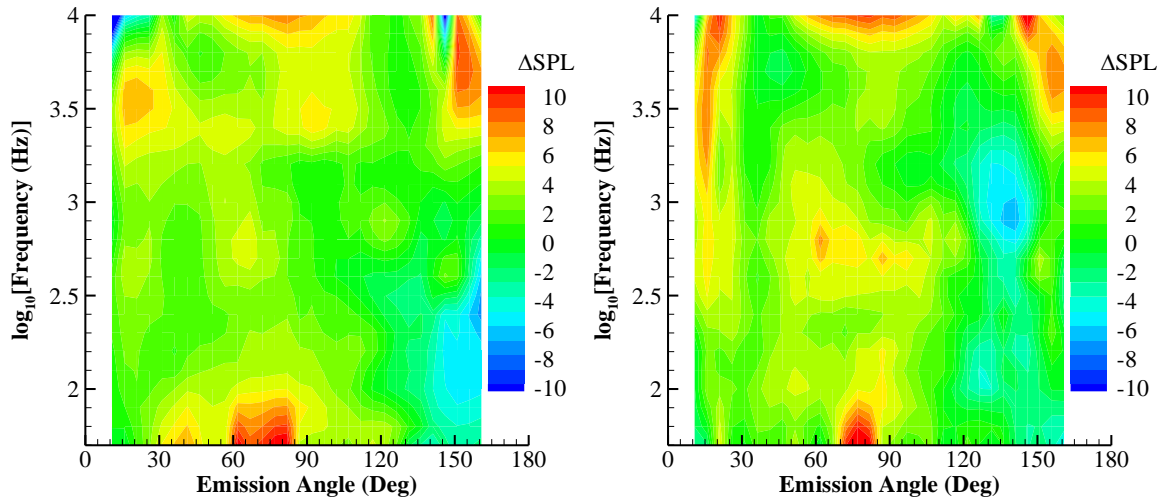


Fig. 10 Prediction accuracy of flap noise spectra at takeoff (left) and landing (right) settings in flyover plane.

For the most important frequencies, between about 100 Hz to 6000 Hz, noticeable overpredictions of up to 6 dB are seen in the angular domain from about 30 to 120 degrees. This is the parametric domain that significantly contributes to the total flap noise. The large amount of overpredictions in this parametric domain significantly affects the total flap noise and calls for major improvement of the prediction method. The cause of these errors is the insufficient modeling of the advanced flap systems in modern aircraft such as the Boeing 787-10 aircraft, which follows the concept of continuous trailing edge architecture where the flaps are all single element and the transition from the inner to the outer flap is made gradually using flaperons that have approximately the same chord length and deployment angle as the flaps. This design feature can be seen in Fig. 1 and is very different from the multielement flap systems in prior aircraft types for which the flap noise model currently in ANOPP-Research was originally developed [3]. The simpler and smoother flap systems not only reduce the number of flap side edges, which correspondingly reduces the number of sources and the noise amplitude, but also smooth the spanwise geometric variations by avoiding abrupt or fully exposed side edges, potentially weakening the source strength and/or altering the far field radiation pattern. Fig. 10 shows that the amount of overprediction varies with frequency and emission angle, as well as the flap settings. Thus, the improvement in the flap noise prediction method calls for amplitude modeling with these parametric variations.

The prediction errors for the flap noise component discussed in the previous paragraphs are summarized in Table 5, listing respectively the domain of the errors in terms of frequency and emission angle, the possible causes of the errors, the potential improvements to correct the errors, and the impact of the potential improvements to the total flap noise prediction.

Table 5 Flap noise prediction error and potential improvement.

Domain	Possible Cause	Potential Improvement	Impact on Component EPNL
High Frequency (above 6000 Hz)	Measurement Uncertainty	No	None
Low Frequency (below 100 Hz)	Flap Chord Length Scaling	Yes	Minor
Kilohertz Range at All Angles	Advanced Flap System Modeling	Yes	Major

The impact of the overpredictions in the flap noise spectra on the total flap noise is illustrated in Fig. 11 in terms of the errors of the noise metric PNL_T as a function of the emission angle, for both the takeoff and the landing settings. The corresponding errors in EPNL for the two cases are respectively 2.7 and 2.6 dB, both significant overpredictions. In both cases, the overpredictions that most significantly affect the EPNL levels are in the range between about 30 to 120 degrees, consistent with the errors in the spectral predictions.

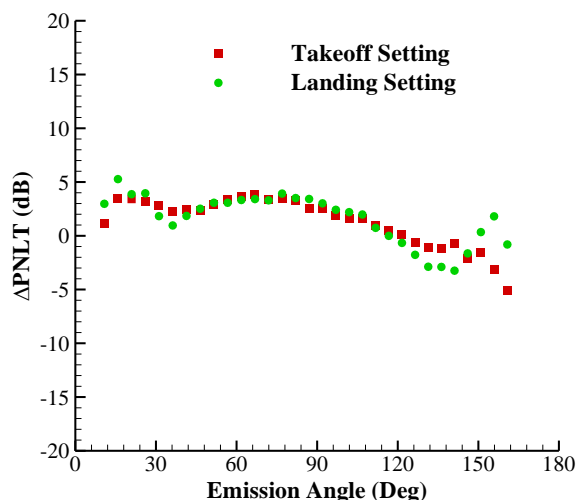


Fig. 11 Prediction errors of flap noise PNL_T in flyover plane.

VI. Trailing Edge Noise

The method for trailing edge noise prediction in ANOPP is the only airframe noise component that has not been updated since the Fink method was implemented [1], [2]. This is mainly because the trailing edge noise is only a minor component for conventional aircraft and has little impact on the total noise. An assessment of the Fink method is included here because the component may have more important contributions to the total noise for some unconventional aircraft configurations, such as the truss braced wing configuration that has longer wingspan than conventional designs [20]. The Boeing 787-10 flight tests provide good quality trailing edge noise data that contain features of modern commercial aircraft related to trailing edge noise, and thus, can help establish the accuracy and applicability of the method.

The Fink method for trailing edge noise prediction is based on the theory of vortex scattering noise by semi-infinite plates. The spectral peaks are calibrated by data of aircraft of early designs. Assumptions made in the method include the simplification of the wings by rectangular plates and the use of the half-dipole directivity known for semi-infinite plates. In the former, the wing area is converted to an equivalent rectangular plate with the wingspan as the length of the plate, which also gives the width of the plate. The plate width is considered as an equivalent chord of the wing, which is used to compute the thickness of the turbulent boundary layer at the trailing edge by the formulas for flat

plate turbulent boundary layer flows. The equivalent chord is also used to determine the frequency of the spectral peak. Under the assumption of half-dipole directivity, the method predicts maximum radiation in the upstream direction and zero noise in the downstream direction. An illustration of the predicted spectra is given in Fig. 12, which plots the 1/3 octave band sound pressure level (SPL) as a function of frequency for three emission angles in the flyover plane. The spectral peaks are usually in the hundred hertz range and are correlated to the equivalent chord length.

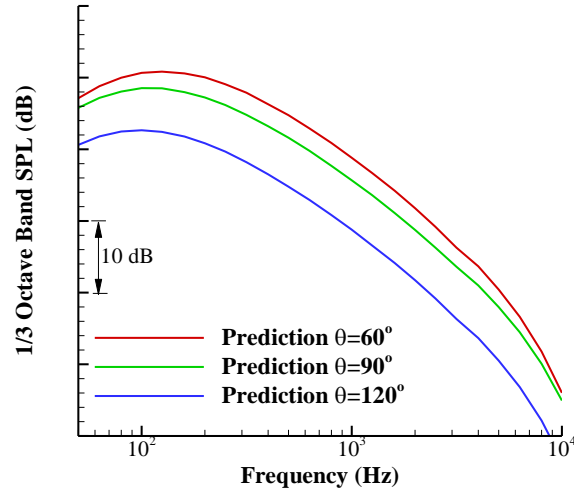


Fig. 12 Illustration of trailing edge noise spectra by Fink method.

The results in Fig. 12 show a decreasing trend in noise levels with increasing emission angle, due to the assumed half-dipole directivity. This is further illustrated in Fig. 13 that plots the overall sound pressure level (OASPL) as a function of the emission angle in the flyover plane. The maximum radiation in the directivity is in the upstream direction of zero emission angle. The levels at very small angles, however, are heavily reduced by the large propagation distances, due to the spherical spreading of the waves and atmospheric absorption. The joint effect of these features then leads to the peak radiation angle for the OASPL around 50 degrees in the forward quadrant.

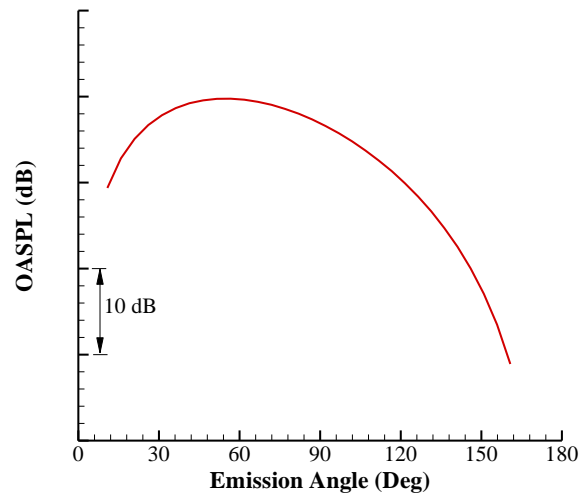


Fig. 13 Illustration of trailing edge noise OASPL by Fink method.

To show the accuracy of the Fink method, the errors of the spectral prediction, compared to the Boeing 787-10 flight test data, are given in Fig. 14, where the errors in the spectral predictions are plotted as a function of both frequency and emission angle in the flyover plane. The prediction errors vary significantly in both frequency and emission angle. For fixed emission angle, the error range in all frequencies can exceed 10 dB, with the smallest error range at the overhead location of 90 degrees emission angle, where the Fink method overpredicts at low frequencies by up to 5 dB and underpredicts, by up to 9 dB, in the mid- and high-frequency domain. For fixed frequency, the

angular dependence is overpredicted in the forward quadrant and underpredicted in the aft quadrant, both significantly by as much as 20 dB at small and large angles.

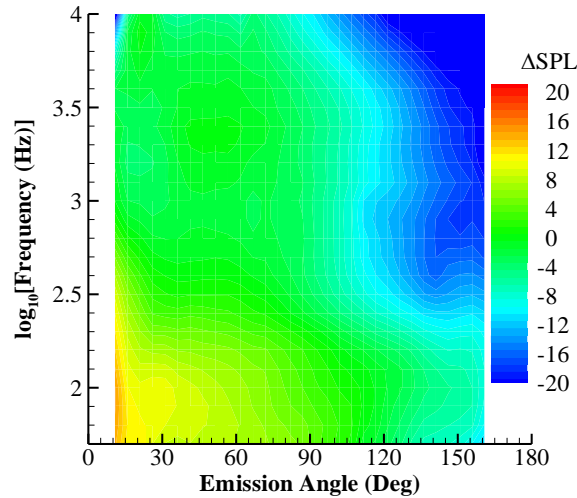


Fig. 14 Prediction error map of trailing edge noise spectra in flyover plane.

The impact of the errors in the spectral prediction on the total trailing edge noise is illustrated in Fig. 15 in terms of the errors in PNL_T as a function of the emission angle. The errors are relatively small within the angular domain from 30 to 60 degrees. At small emission angles, there are significant overpredictions of up to 6 dB, but the contributions from these angles are small because of the low noise levels. At angles above about 60 degrees, there are significant underpredictions and the amount of underprediction increases with the emission angle. This has a noticeable effect on the EPNL level, which has an error of -2.3 dB, significantly underpredicting the test data.

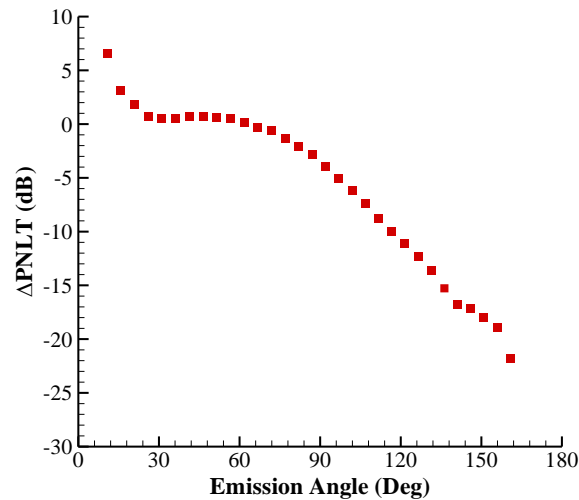


Fig. 15 Prediction errors of trailing edge noise PNL_T in flyover plane.

The errors of the Fink method for the trailing edge noise component, shown in the above figures, can be attributed to the assumptions in the method, discussed earlier in this section. The first is the use of a rectangular plate to represent a wing, which gives a single equivalent chord length for the wing, and thus, a single boundary layer thickness and a single peak frequency, leading to a spectrum of a narrow hump with rapid falloff. However, Boeing 787-10 aircraft, and any other modern aircraft, have highly tapered wings with significantly varying chord length. Thus, the trailing edge noise from real aircraft can be expected to have more broad spectra due to the multiple peak frequencies related to the multiple chord lengths. This explains the underpredictions at mid and high frequencies above the spectral peak. The overpredictions around the spectral peaks are also due to this rectangular plate simplification, because it increases the spanwise extent of the wing segment with chord length close to the width of the rectangular plate. The trend of the prediction errors in the spatial domain as a function of the emission angle is related to the use of the half-dipole

directivity, suitable to semi-infinite plates but not accurate for aircraft wings that have finite chord lengths. The model assumes an infinitely large reflecting plate in the upstream direction, causing the overpredictions at forward angles that are only mitigated by the decay of noise amplitudes at large propagation distances. In the downstream direction, the model underpredicts the noise levels, which, together with the decrease of noise levels due to propagation, leads to the very low levels at aft angles shown in Fig. 15. The use of flat plate models for the calculation of the turbulent boundary layer may also lead to errors in the noise amplitudes for the trailing edge noise of aircraft wings and high-lift elements. In this case, the surfaces are curved, and the turbulent boundary layer flows are affected by the presence of other high-lift elements.

The analyses of the prediction errors for the trailing edge noise component discussed in the previous paragraphs are summarized in Table 6, showing the domains of the errors in terms of frequency and emission angle, the possible causes of the errors, the potential improvements to correct the errors, and the impact of the potential improvements to the total trailing edge noise prediction.

Table 6 Trailing edge noise prediction error and potential improvement.

Domain	Possible Cause	Potential Improvement	Impact on Component EPNL
Spectrum	Single Length Scale	Yes	Major
Directivity	Semi-Infinite Plate Model	Yes	Major
Amplitude	Flap Plate Boundary Layer Flow	Yes	Major

VII. Comparison with Other Methods

While all three generations of the prediction methods for the major airframe noise components are implemented in the ANOPP framework, only the first two, ANOPP-Fink and ANOPP-BAF, are available in the current public version. To demonstrate the overall accuracy of the three generations of airframe noise prediction methods and to illustrate the progress of the method development, Fig. 16 shows the prediction errors, compared with the Boeing 787-10 test data, in the noise metric of PNLT for the landing gear noise component. The errors are plotted as a function of emission angle, for the three methods in ANOPP, at landing settings. The improvement in the prediction accuracy from the early Fink method to the method of BAF, and then to the current version, is clearly seen from the comparisons. Within the angular domain from 60 to 120 degrees, all three methods have relative consistent respective accuracy, with about 3 dB for the Fink method and about 1 dB for the other two. Outside this angular range, however, the accuracies diverge, with the Fink method significantly underpredicting and the BAF method noticeably overpredicting. The directivity pattern of the gear noise is not captured by the Fink method.

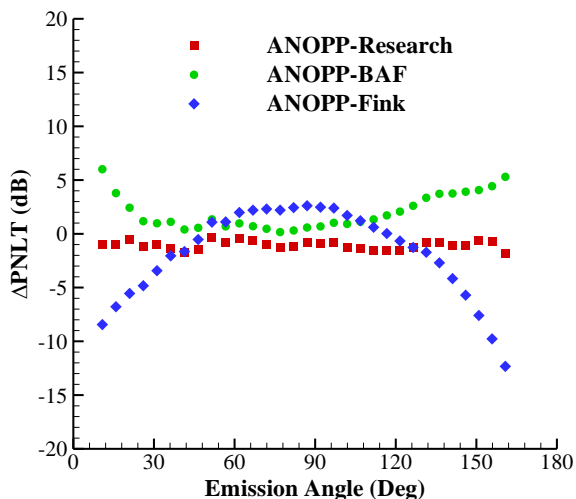


Fig. 16 Comparison of gear noise prediction accuracy in PNLT in flyover plane at landing setting.

One of the major improvements of the current generation of methods is the expanded functionalities and the reduced dependence on test data calibration. The earlier methods are all heavily calibrated by test data at typical

landing settings. Thus, the prediction errors shown in Fig. 16 are noticeable, but can still be considered acceptable, at this specific flight condition. The aircraft configuration and/or the high-lift system can deviate from the conventional aircraft design and/or from the typical landing settings in many applications, requiring the prediction method to be versatile and robust in configuration variations. This is illustrated in Fig. 17, which plots the prediction errors in PNLT of the landing gears noise component from the three methods for a cruise wing. The cruise wing configuration will probably never be used for landing. It is used here only to demonstrate the capabilities of the prediction methods in dealing with configuration variations. In this case, the latest method, the ANOPP-Research, shows good accuracy. On the other hand, the Fink method significantly underpredicts the data for almost all the emission angles with an incorrect directivity pattern. The BAF method almost uniformly overpredicts by about 2 dB, which is also seen in Fig. 16 at landing settings. This is due to the use of a reflection model in the method, derived from a large flat plate, which overpredicts the reflection by the aircraft. This is one of the improvements from ANOPP-BAF to ANOPP-Research. The latter has the capability of calculating the reflection effects with the aircraft geometry.

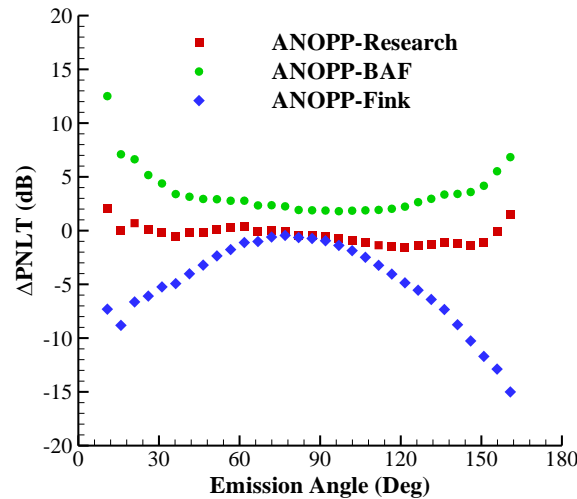


Fig. 17 Comparison of gear noise prediction accuracy in PNLT in flyover plane for cruise wing.

The comparisons of the prediction accuracies of the three methods for the slat noise component are given in Fig. 18, which plots the errors in PNLT as a function of emission angle, at landing settings in the flyover plane. The trends in ANOPP-BAF and ANOPP-Research are similar, with the latter slightly underpredicting. The Fink method does not capture the directivity pattern, which, together with other incorrect assumptions in the method, leads to the large errors shown in the figure.

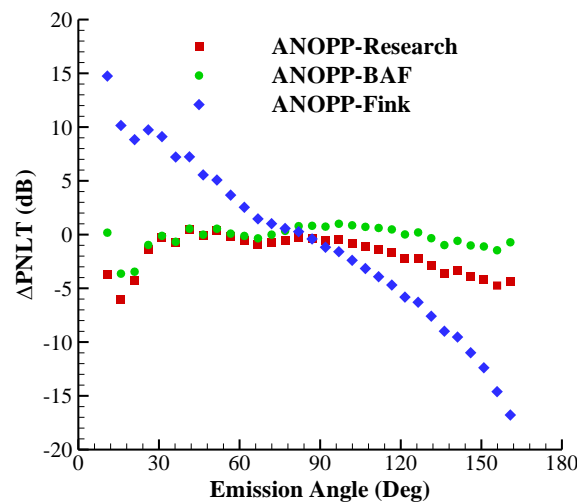


Fig. 18 Comparison of slat noise prediction accuracy in PNLT in flyover plane at landing setting.

Similarly, the comparisons of the prediction accuracies of the three methods for the flap noise component are given in Fig. 19, plotting the errors in PNLT as a function of emission angle at landing settings in the flyover plane. Overall, all three methods overpredict the Boeing 787-10 data. For the ANOPP-BAF and the ANOPP-Research methods, the reasons for the overprediction are the same and have been discussed in an earlier section, namely, the inadequate modeling of the advanced flap system for this aircraft. The causes of the errors in the Fink method are similar to its slat noise method, namely, the incorrect modeling of the source mechanisms together with other incorrect assumptions.

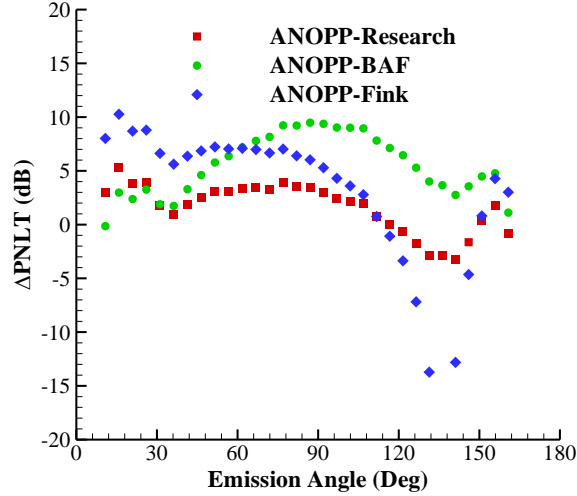


Fig. 19 Comparison of flap noise errors in PNLT in flyover plane.

VIII. Conclusions

In this paper, an assessment of the airframe noise prediction methods in ANOPP has been presented, by using the flight test data of the Boeing 787-10 aircraft, to illustrate the accuracy of the methods and to identify potential improvements to further mature the prediction methods. Though comparisons have been presented between various previous generations of the prediction methods in ANOPP, to demonstrate the progress of the development of the methods, the focus of the assessment has been the current generation of methods, implemented as ANOPP-Research, which will also be the basis for future improvements.

Satisfactory accuracy has been demonstrated for the landing gear and the slat noise component, with only minor potential improvements identified. One such improvement is the definition of the characteristic length scales used in the Strouhal number scaling for low frequency noise, for the landing gear wheel noise and the slat cove noise, which can potentially improve the predictions at frequencies below about 100 Hz. The improvement would be minor since the low frequency noise is lightly weighted in the noise certification metrics. Another potential minor improvement is identified for the landing gear noise component as the interactions between the gear wake flow and the trailing edges of the wings and/or flaps, which are not modeled in the current prediction method. This would affect the mid-frequency range at some emission angles away from the overhead position, and thus, represent a minor improvement for the total landing gear noise. For slat noise, the directivities of the gap noise and the bracket noise are also identified as potential minor improvements, essentially at large emission angles.

The most noticeable feature in the assessment of the flap noise prediction method has been the overpredictions, compared with the flight test data, in a wide range of frequencies and emission angles, overwhelming the satisfactory accuracy in the prediction of various parametric trends. The cause of the overpredictions has been discussed, resulting from the inadequate modeling of the advanced flap systems of modern aircraft such as the Boeing 787-10 aircraft. This has been identified as a major potential improvement, to meet the needs for current and future generations of aircraft.

The need for major improvement has also been identified for the trailing edge noise component. The predictions of the noise spectrum, the far field directivity, and the noise amplitude of the trailing edge noise have shown large errors, attributed to the incorrect assumptions in the prediction method. While the trailing edge noise component still remains a minor component for conventional aircraft, it may play an increasingly more important role for unconventional aircraft, calling for a more accurate prediction method.

Acknowledgments

The extraordinary support and funding of this research by the NASA Advanced Air Transport Technology Project is gratefully acknowledged. The exceptional efforts of The Boeing Company and the Boeing ecoDemonstrator Program are gratefully acknowledged for executing this challenging test under difficult circumstances. Members of the Propulsion Airframe Aeroacoustics and Aircraft System Noise Team of the Aeroacoustics Branch at NASA Langley Research Center are also thanked for their support.

References

- [1] Fink, M. R., "Approximate Prediction of Airframe Noise," *Journal of Aircraft*, Vol. 13, No. 11, pp. 833–834, 1976. doi:10.2514/3.58718.
- [2] Fink, M. R., "Airframe Noise Prediction Method," FAA-RD-77-29, March 1977.
- [3] Fink, M. R., "Noise Component Method for Airframe Noise," AIAA Paper 1977-1271, 4th AIAA Aeroacoustics Conference, Atlanta, Georgia, October 1977. doi:10.2514/6.1977-1271.
- [4] Guo, Y., "Aircraft Flap Side Edge Noise Modeling and Prediction," AIAA Paper 2011-2731, 17th AIAA/CEAS Aeroacoustics Conference, Portland, Oregon, June 2011. doi:10.2514/6.2011-2731.
- [5] Guo, Y., "Slat Noise Modeling and Prediction," *Journal of Sound Vibration*. Vol. 331, pp. 3567-3586, 2012. doi:10.1016/j.jsv.2012.03.016
- [6] Guo, Y., "Effects of Local Flow Variations on Landing Gear Noise Prediction and Analysis," *Journal of Aircraft*, Vol. 47, No. 2, pp. 383–391, 2010. doi:10.2514/1.43615.
- [7] Block, P. J. W., "Assessment of Airframe Noise," *Journal of Aircraft*, Vol. 16, No. 12, pp. 834-841, 1979. doi: 10.2514/3.44641.
- [8] Dobrzynski, W., "Almost 40 Years of Airframe Noise Research: What Did We Achieve?" *Journal of Aircraft*, Vol. 47, No. 2, pp. 353-367, 2010. doi: 10.2514/1.44457.
- [9] Pott-Pollenske, M., Dobrzynski, W., Buchholz, H., Guerin, S., Saueressig, G. and Finke, U., "Airframe Noise Characteristics from Flyover Measurements and Prediction," AIAA Paper 2006-2567, 12th AIAA/CEAS Aeroacoustics Conference, Cambridge, Massachusetts, May 2006. doi:10.2514/6.2006-2567.
- [10] Pott-Pollenske, M., Dobrzynski, W., Buchholz, H., Gehlhar, B. and Walle, F., "Validation of a Semiempirical Airframe Noise Prediction Method Through Dedicated A319 Flyover Noise Measurements," AIAA Paper 2002-2470, June 2002. doi:10.2514/6.2002-2470.
- [11] Dahl, M., "A Process for Assessing NASA's Capability in Aircraft Noise Prediction Technology," AIAA Paper 2008-2813, 14th AIAA/CEAS Aeroacoustics Conference, Vancouver, British Columbia, May 2008. doi:10.2514/6.2008-2813.
- [12] Burley, C., Brooks, T., Humphreys, W. and Rawls, J., "ANOPP Landing Gear Noise Prediction Comparisons to Model-Scale Data," AIAA Paper 2007-3459, 13th AIAA/CEAS Aeroacoustics Conference, Rome, Italy, May 2007. doi:10.2514/6.2007-3459.
- [13] Thomas, R.H., Guo, Y., Clark, I.A., and June, J.C., "Propulsion Airframe Aeroacoustics and Aircraft System Noise Flight Research Test: NASA Overview," Paper accepted to the 28th AIAA/CEAS Aeroacoustics Conference, Southampton, United Kingdom, June 2022.
- [14] Czech, M.J, Thomas, R.H., Guo, Y., June, J.C., Clark, I.A., and Shoemaker, C., "Propulsion Airframe Aeroacoustics and Aircraft System Noise Flight Test on the ecoDemonstrator 2020 – Boeing 787 Testbed Aircraft," Paper accepted to the 28th AIAA/CEAS Aeroacoustics Conference, Southampton, United Kingdom, June 2022.
- [15] Guo, Y., "A statistical model for landing gear noise prediction," *Journal of Sound and Vibration*, Vol. 282, pp. 61-87, 2004. doi:10.1016/j.jsv.2004.02.021.
- [16] Guo, Y., "A Semi-Empirical Model for Aircraft Landing Gear Noise Prediction," AIAA Paper 2006-2627, 12th AIAA/CEAS Aeroacoustics Conference, Cambridge, Massachusetts, May 2006. doi:10.2514/6.2006-2627.
- [17] Guo, Y., Burley, C. and Thomas, R. H., "Landing Gear Noise Prediction and Analysis for Tube-And-Wing and Hybrid-Wing-Body Aircraft," AIAA Paper 2016-1273, 54th AIAA Aerospace Sciences Meeting, San Diego, California, January 2016. doi:10.2514/6.2016-1273.
- [18] Guo, Y., Burley, C. L. and Thomas, R. H., "Modeling and Prediction of Krueger Device Noise," AIAA Paper 2016-2957, 22nd AIAA/CEAS Aeroacoustics Conference, Lyon, France, June 2016. doi: 10.2514/6.2016-2957.
- [19] Thomas, R. H., Burley, C. L. and Olson, E. D. "Hybrid Wing Body Aircraft System Noise Assessment with Propulsion Airframe Aeroacoustic Experiments," *International Journal of Aeroacoustics*, **11** (3+4), 369-410, 2012. doi:10.1260/1475-472X.11.3-4.369.
- [20] June, J., Thomas, R. H., Guo, Y., "System Noise Technology Roadmaps for a Transonic Truss-Braced Wing and Peer Conventional Configuration," Paper accepted to the 28th AIAA/CEAS Aeroacoustics Conference, Southampton, United Kingdom, June 2022.
- [21] Guo, Y. and Thomas, R. H., "On Aircraft Trailing Edge Noise," AIAA Paper 2019-2610, 25th AIAA/CEAS Aeroacoustics Conference, Delft, The Netherlands, May 2019. doi:10.2514/6.2019-2610.
- [22] Smith, M., Carrilho, J., Molin, N., Piet, J. and Chow, L., "Modelling of Landing Gear Noise with Installation Effects," AIAA Paper 2007-3472, 13th AIAA/CEAS Aeroacoustics Conference, Rome, Italy, May 2007. doi:10.2514/6.2007-3472.

- [23] Guo, Y., Yamamoto, K. and Stoker, R. W., “Experimental Study on Aircraft Landing Gear Noise,” *Journal of Aircraft*, Vol. 43, No. 2, pp. 306–317, 2006. doi:10.2514/1.11085.
- [24] Oerlemans, S. and Pott-Pollenske, M., “An Experimental Study of Gear Wake/Flap Interaction Noise,” AIAA Paper 2004-2886, 10th AIAA/CEAS Aeroacoustics Conference, Manchester, Great Britain, May 2004. doi:10.2514/6.2004-2886.
- [25] Pott-Pollenske, M. and Almoncit D., “A Study on Landing Gear Wake – Flap Interaction Noise,” AIAA Paper 2017-3692, 23rd AIAA/CEAS Aeroacoustics Conference, Denver, Colorado, June 2017. doi: 10.2514/6.2017-3692.